ELSEVIER

Thermochimica Acta 284 (1996) 85–102

thermochimica acta

Para-substituted polystyrenes: Stress relaxation, creep, dynamic mechanical and dielectric analyses[1]

Hang Gao, Julie P. Harmon *

Department of Chemistry, University of South Florida, 4202 E. Fowler Ave., Tampa, Fl 33620-5250, USA

Abstract

The effects of methyl, ethyl, *n*-propyl and *t*-butyl para-substituents on relaxations in polystyrene are characterized via multiple thermal techniques. It is shown that the glass transition temperature T_g can be readily obtained from stress relaxation and creep data by locating the intersecting point of the Arrhenius and WLF curves on the logarithm of the shift factor a_T vs. temperature plots. The T_g thus obtained from stress relaxation data is correlated well with literature values obtained by isochronal dilatometry. The processes of creep and stress relaxation show two regions of distinct molecular motion patterns with different activation energies determined. Rubbery plateaus for stress relaxation moduli due to chain entanglements are observed for polystyrene, poly (*p*-methyl styrene) and poly (*p*-*t*-butyl styrene). The flexural storage moduli E' for the three polymers show a density dependency, which is correlated by the Rao function. The peak width of loss modulus E'' is affected by the molecular weight distribution of each polymer. Two weak sub-glass transition temperature transitions, β and γ, are also observed from dynamic mechanical analysis. The variations in the glass transition temperature and activation energy from dielectric analysis are analyzed with regard to steric hindrance resulting from different alkyl groups.

Keywords: Polystyrene; Stress relaxation; Creep

1. Introduction

Polystyrene and its derivatives are versatile industrial polymers as well as model polymers for theoretical studies. Para-alkyl substitution of polystyrenes was first

* Corresponding author.

[1] Presented at the 24th North American Thermal Analysis Society Conference, San Francisco, CA, U.S.A., 10–13 September 1995

PII: S0040-6031(95)02921-8

systematically studied by Overberger et al. [1] and later by others [2–7]. Referactive indexes and refractometric transition temperatures were determined. The glass transition temperatures via differential scanning calorimetry, gas transport properties and radiation effects of para-alkylated polystyrenes were further studied by Puleo et al. [8] and Schuenemann [9]. They found that modification of the side groups on the para-site of polystyrene resulted in changes in the glass transition temperatures, in gas permeability, and in radiation resistance. The high refractive index of the polystyrene system due to the presence of the phenyl group and the relative ease in the modification of its chemical structure make polystyrenes suitable optical fiber materials [10–13]. The ever-expanding use and increasing demand for better properties in polystyrene has made further understanding of the viscoelastic properties of alkylated polystyrene systems very desirable and this is the focus of this research.

This study employs the thermal analysis techniques of stress relaxation, creep, dynamic mechanical and dielectric analyses. The combined techniques probe structural transitions and molecular mobilities of the substituted polystyrenes from multi-angles. The polymers examined include polystyrene (PS), poly(*p*-methyl styrene) (PMS), poly (*p*-ethylstyrene) (PES), poly(*p*-*n*-propylstyrene) (PPS) and poly (*p*-*t*-butylstyrene) (PTBS). Molecular weights, polydispersities and DSC glass transition temperatures of these polymers are listed in Table 1.

Stress relaxation and creep are very effective methods in the study and prediction of the long term behaviors of polymers [14,15]. A master curve is typically generated from short-term experiments at elevated temperatures. The time–temperature equivalency of viscoelastic materials allows the data obtained from high temperatures to be applied to long-term situations at low temperature, e.g., the end use temperature. These properties are typically impractical to acquire in the limited time of product development and testing. The time–temperature superposition principle has been used for a long time [16–20]. In 1955, Williams et al. first correlated the reference temperature to the glass transition temperature [20]. The WLF equation was further derived from the free volume theory of polymers above the glass transition temperature [21]. Adam and Gibbs introduced molecular kinetics to polymers and the WLF equation become a natural consequence of their treatment [22]. Matsuoka and Quan further developed a conformational relaxation model [23,24]. It has been shown that the parameters in the WLF equation are not necessarily universal and one of the two parameters, C_2, is temperature dependent. Yet for convenience, the glass transition temperature, T_g, or $T_g + 50$ K has been chosen as a reference temperature [15]. However, due to the kinetic

Table 1
Molecular weights and DSC glass transition temperatures of polymers studied

Polymers	Abbreviation	M_w	M_n	M_w/M_n	DSC T_g (5°C min^{-1})
Polystyrene	PS	425,000	203,000	2.09	96.7
Poly(*p*-methylstyrene)	PMS	398,000	187,000	2.13	101.3
Poly(*p*-ethylstyrene)	PES	334,000	77,000	4.34	64.8
Poly(*p*-*n*-propylstyrene)	PPS	316,000	96,000	3.29	38.5
poly(*p*-*t*-butylstyrene)	PTBS	303,000	131,000	2.31	125.6

nature of the glass transition process, T_g is not a constant and varies greatly with test conditions and test methods [15,25]. If the experiment is performed in hours or days, the glass transition temperature will be lower. Thus a "rate-independent" glass transition temperature, such as dilatometric [26,27], or slow ramp rate DSC [28,29] has been normally used as reference temperature, although a variation of 2–3 K is still observed by these methods [26]. Based on the understanding that stress relaxation and creep are kinetic processes with activation barriers [26,30] and also based on stress relaxation and creep data presented here for the polystyrenes, a more convenient and direct way to determine the glass transition temperature is proposed. This T_g can be used as a reference temperature for stress relaxation and creep experiments. Two modes of molecular motions for stress relaxation and creep are identified and their activation energies are determined for these processes.

Dynamic mechanical analysis is another versatile, sensitive and widely used method to study the viscoelastic properties of polymeric materials [14, 26]. The dynamic storage modulus, E', and loss modulus, E'', are among the most basic of all mechanical properties, and their importance in any structural property relationship is well applied. There are a large number of literature references about the dynamic mechanical properties of polystyrene [31–39]; however comparative studies on para-alkylated polystyrenes are scarce. The current study of dynamic mechanical properties focuses on polystyrene, poly(*p*-methyl styrene) and poly(*p*-*t*-butyl styrene). Dielectric analysis is yet another powerful method in probing into the molecular mobility and structural relaxations of polymers [40–42]. Many interesting results from dielectric analysis have been published for polystyrene, even though styrene does not have a strong dipole moment. Labeling polystyrene with groups of high dipole moments in the forms of end group, pendant group, and as guest molecules has been successfully used to understand the microscopic behavior of polystyrenes [43–49]. Our dielectric study greatly advances the understanding of the glass transition process in the polystyrenes examined.

2. Experimental

The monomers, styrene, *p*-methyl styrene and *p*-*t*-butyl styrene were obtained from Aldrich Chemicals. Inhibitors (4-*tert*-butyl catechol) were removed by passing the liquids through a 10-cm alumina powder column. Monomers were then polymerized by free radical bulk polymerization with the peroxide, 1,1-di(*t*-butylperoxy)-3,3,5-trimethylcyclohexane. poly(*p*-ethyl styrene) and poly (*p*-*n*-propyl styrene) were prepared and free-radical bulk-polymerized with AIBN by Schuenemann [9]. Gel permeation chromatography (ISCO 2350) was used to determine the polystyrene equivalent molecular weights. DSC experiments were performed on TA Instruments' DSC 2920. All DSC samples, weighing about 10 mg, were encapsulated in standard aluminum DSC pans. The heating rate was 5°C min^{-1}. Polymers studied in this paper are listed in Table 1. Creep and stress relaxation experiments were carried out on a TA Instruments DMA 983 thermal dynamic mechanical analyzer equipped with creep and stress relaxation modes respectively. Samples were hot-pressed to sheets, of 35 × 12 × 1 mm^3 in size. They were equilibrated at about 30°C and then kept isothermal for 20 min,

followed by another 20 min recovery period before moving to a new temperature. A step temperature of 5°C was employed. Time–temperature superposition, and WLF and Arrhenius equation fitting were performed with the TA DMA Superposition program. Creep and stress data obtained at one temperature were horizontally shifted to match smoothly with the curve at a reference temperature. Vertical shift was not used. Dynamic mechanical analysis was done on a TA Instruments DMA tester DMA 983 in the fixed frequency mode. Oscillation frequency ranged from 0.1 to 10 Hz with an amplitude of 0.4 mm; a heating rate of 2°C min^{-1} was applied. A temperature range from −150°C to about 150°C was swept for each sample. A DEA 2790 from TA Instruments was used to record the dilectric spectra of all the polymers under study. Samples were hot-pressed into disks 0.75 mm thick and 20 mm in diameter, sandwiched in gold-plated parallel plates with 250 N force, and heated from −150°C to 200°C at 3°C min^{-1}. Applied frequencies ranged from 0.1 to 100,000 Hz.

3. Results and discussion

3.1. Glass transition temperature and activation energy from creep and stress relaxation

It is known that the creep and stress relaxation behavior above the glass transition temperature for many amorphous polymers can be superposed and the shift factor a_T follows the WLF equation [14, 15, 19, 20, 26].

$$\log a_T = \frac{C_1(T - T_0)}{C_2 + (T - T_0)} \tag{1}$$

where C_1, C_2 are constants and T_0 is a reference temperature. A typical range is between T_g and $T_g + 100$ K. The reference temperature is chosen to be the mid-point of this range and is known as standard reference, T_s. Due to the difficulties in obtaining a true "rate-independent" glass transition temperature, a dilatometric glass transition temperature is often used [26], even though a variation of 2–3 K in the glass transition temperature will still be expected for long-term experiments. Many studies used glass transition temperatures from DSC [28,29] instead. Thus test conditions and sample conditions can vary appreciably because of the need to determine the reference temperature for the WLF equation separately via a different instrumental technique. The constants, C_1 and C_2 do not have a constant nature [22,23]. The current study (Figs. 1 and 2) shows that the glass transition process can be observed within the creep and stress relaxation experiments. This means that using the glass transition temperature from other experiments may not be necessary. This method, the authors believe, is a more meaningful and convenient treatment of stress relaxation and creep data with regard to glass transition processes. In a stress relaxation study by Shimo and Nagasawa [50], it was noted that shift factors below T_g started to drift away from the WLF equation; they attributed this phenomenon to the difficulty in shifting the flat log E vs. log t curve in the glassy region. This drifting of shift factors was also noted by

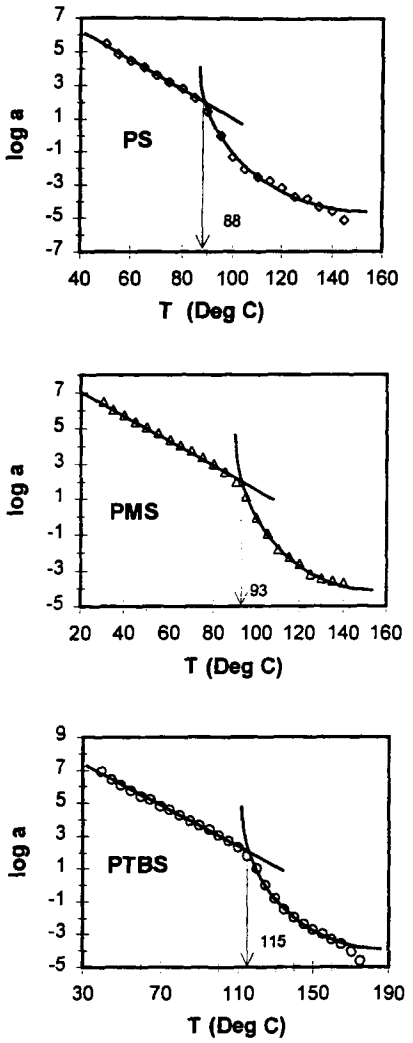

Fig. 1. Plots of the logarithm of the stress relaxation shift factor a, $\log a$, vs. temperature T, for PS, PMS and PTBS. Glass transition temperatures are obtained from the intersecting points of the Arrhenius curves below T_g and the WLF curves above T_g.

Rusch [51] and Nielsen [15]. As can be seen in Figs. 1 and 2, the scattering of shift factors is not significant at all in our creep and stress relaxation experiments. Fig. 1 shows the plots of $\log a_T$ vs. $\log t$ for PS, PMS and PTBS obtained from stress relaxation experiments and Fig. 2 shows those from creep experiments. It can be clearly seen that there are two basic regions for all three polymers. The high-temperature side shows clear curvature and is well-fitted to the WLF equation. However, on the low-temperature side, the data follow Arrhenius behavior. Halsey, et al. [52] assumed

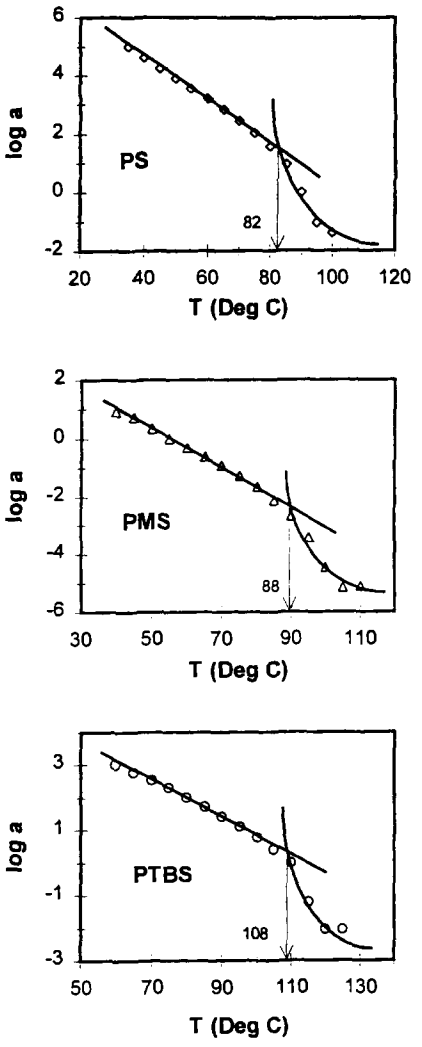

Fig. 2. Plots of the logarithm of the creep shift factor a, log a, vs. temperature T for PS, PMS and PTBS. Glass transition temperatures are obtained from the intersecting points of the Arrhenius curves below T_g and the WLF curves above T_g.

that the deformation of a polymer was a thermally activated rate process involving the motion of segments of chain molecules over potential barriers, whose frequency v depends on the ease with which a chain segment can overcome a potential energy barrier of height ΔH

$$v = v_0 \exp\left[-\frac{\Delta H - \beta\sigma}{RT}\right] \tag{2}$$

where ΔH is a potential energy barrier, or activation enthalpy, and σ is the stress on the sample from the creep or stress relaxation experiment. A linear shift of the energy barrier is assumed with a coefficient β that has the dimensions of volume. The authors believe that a negative sign should be used symbolically to indicate that the applied stress generally helps the forward structural relaxation process of polymers and thus lowers the energy barrier. When the external stress is small enough, the $\beta\sigma$ term can be neglected, leaving the intrinsic enthalpy as the major energy barrier during structural relaxation in creep and stress experiments. In the glassy state, due to the limited space available for structural relaxation, the activation entropy, ΔS, is neglected as indicated in Ref. [53,54]. To determine the glass transition from creep and stress relaxation data, an Arrhenius plot, log a_T vs. $1/T$, for the low-temperature side was empolyed, while on the high-temperature side, the WLF equation was employed. The intersecting point defines the glass transition temperatures for stress relaxation and creep experiments. Table 2 lists the glass transition temperatures thus obtained for both stress relaxation and creep experiments. Activation energies on the low and high side of the glass transition temperature were also calculated from creep data using Eq. 2. The WLF equation was fitted to stress relaxation data above the glass transition temperature. Since too few data points above T_g were available from creep experiments, no reliable WLF equation fits could be obtained from creep data. However, the intersecting point can still be obtained from the plot without great difficulty (Fig. 2). Parameters C_1 and C_2 from stress relaxation are also listed on Table 2. The activation energy at the high-temperature side from stress relaxation is calculated by using the derivative of the WLF equation at T_g [55]

$$\Delta H = -2.303\,(C_1/C_2)R\,T_g^2 \tag{3}$$

It is noted that the glass transition temperatures measured from creep are even lower than those from stress relaxation , by 5–7°C. This indicates that large-scale segmental movement represented by the glass transition can begin at even earlier stages in creep experiments. The isochronal dilatometric glass transition temperature for polystyrene reported by and Lee and McGarry [27] is 96.8°C for 1 min. and 88.7°C for 50 h. The latter T_g, 88.7°C, is a very long-term experimental value and it matches very well with our T_g at 88°C from stress relaxation. Yet it took considerably less time (50–60 min for

Table 2
Energy barriers for creep and stress relaxtion processes

Polymers	Creep			Stress			WLF	
	ΔH_{C^-}	ΔH_{C^+}	T_g	ΔH_{S^-}	ΔH_{S^+}	T_g	C_1	C_2
PS	37	101	82	44	129	88	8.3	38.2
PMS	34	111	88	36	135	93	6.7	30.4
PTBS	34	129	108	34	119	115	8.1	46.9

Key: The subscript "C" represents creep and "S" stress relaxation; "+" represents above T_g process and "−" below T_g process.

one data point) to acquire in our experiments compared to 50 h for isochronal dilatometry. The activation energies from both creep and stress experiments are about 33–34 kcal mol^{-1}. This activation energy corresponds well to the isobaric stress relaxation activation energy of 132 kJ mol^{-1} (32 kcal mol^{-1}) obtained by Gol'dman [30] in his study of the energetics of poly(methylmethacrylate) which has typically a glass transition temperature at about 100°C [56], close to that of polystyrene (Table 1). No similar activation energy from stress relaxation and creep are available for polystyrene for comparison. However, the authors believe that the relatively low activation energy compared with the activation energy of 80–86 kcal mol^{-1}, from dynamic mechanical and dielectric data [40,41] and also with our own dielectric data 77 kcal mol^{-1} (Table 7, below), indicates an intramolecular conformation of several monomer units that gives rise to this process. The independent local motion of monomer unit side groups is excluded since it typically has an activation energy of the magnitude of 7–8 kcal mol^{-1} [53]. The value 33–44 kcal mol^{-1} is not large enough to involve large-scale main-chain cooperative movement. On the high-temperature side, activation energies are higher than 100 kcal mol^{-1}. With an increase in temperature, the activation energy (the derivative of the log a_T vs. $1/T$curve, $\Delta H = (-2.303\ C_1\ C_2)\ RT^2/(C_2 + T - T_g)^2$ [55]) tends to decrease [23,24,55]. This indicates that segmental sliding is the major mode of movement above the glass transition temperature. This sliding motion requires cooperative motion of larger segments of the main chain [23,24,26], as the high activation energies indicate. Stress relaxation master curves for the polymers are shown in Fig. 3 and the master curves from creep are shown in Fig. 4. The rubbery plateaus [15] due to long chain entanglement are noted at around 250 MPa for stress relaxation flexural moduli and are very close for all polymers studied.

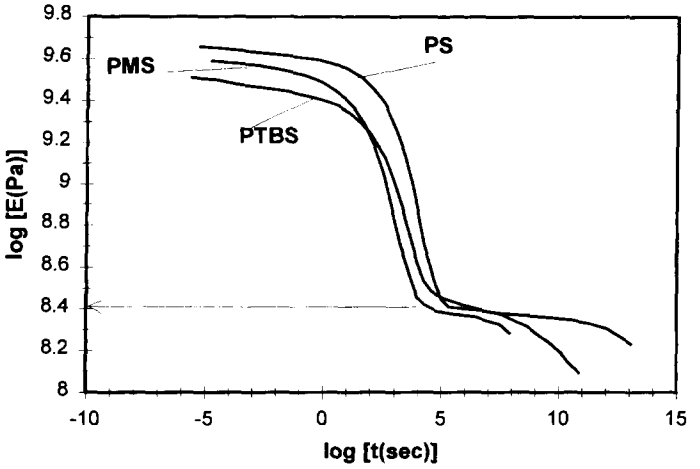

Fig. 3. Master curves for PS, PMS and PTBS from stress relaxation experiments. Rubbery plateaus are observed as indicated by the dashed line.

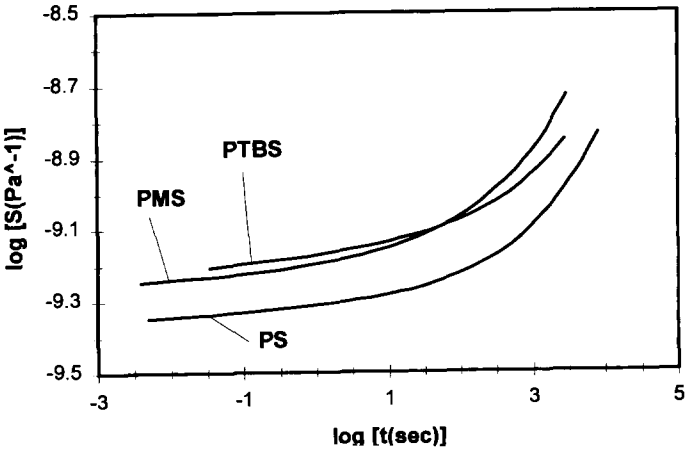

Fig. 4. Master curves for PS, PMS and PTBS from creep experiments.

3.2. *Transitions and the activation energies by dynamic mechanical analysis*

The dynamic mechanical flexural modulus E^* is composed of two parts, the storage modulus E', and the loss modulus E''. They are related by the equation

$$E^* = E' + iE'' \tag{4}$$

E' measures the elastic properties of polymers, and E'' characterizes the viscous properties. Fig. 5 shows the flexural storage modulus of PS, PMS and PTBS from

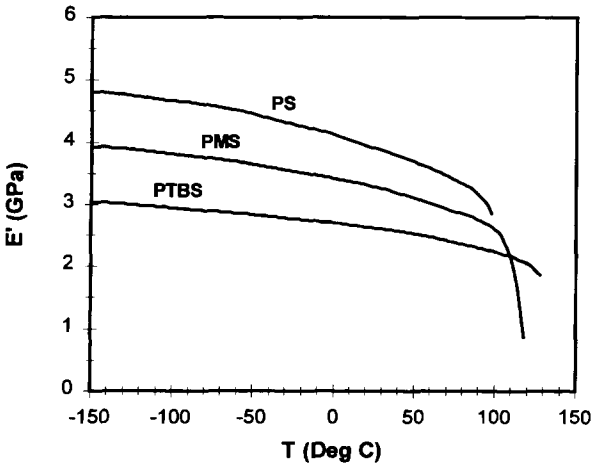

Fig. 5. Flexural storage modulus E' vs. temperature for PS, PMS and PTBS from dynamic mechanical analysis at 1 Hz and heating rate of 2°C min^{-1}.

−150°C to temperatures before the glass transition temperature. With the increase in temperature, the storage moduli for all three polymers drop steadily until just before glass transition temperatures where a larger decrease is offset due to the ease of structural rearrangement. Differences in storage moduli among the three were noted. Table 3 lists the densities and E values for the three polymers at 25°C. Obviously, this difference results from the difference in density which indicates the average number of polymer chains per unit volume that undergo the flexural change during dynamic testing. This trend can be represented by Rao's equation [57,58]

$$E = \rho(U/V)^6 \tag{5}$$

where ρ is density, U is the Rao function and V is the molar volume. From loss modulus vs. T plots, the glass transition, β-transition and γ-transition were recorded for all three polymers. Fig. 6 shows the glass transition for three polymers. The trend in polydispersity matches the half-height width of loss peaks as noted in Table 4. It is known that the distribution of molecular weight of polymers contributes to multiple relaxations around the glass transition regions [40,41]. The half-height width also increases with the size of the pendant group. Large pendant groups tend to decrease the homogeneity of chain packing.

Table 3
Density and flexural modulus of the polymers at 20°C

Polymer	Density [8]/(g cm^{-3})	E'/GPa
PS	1.048	4.0
PMS	1.009	3.4
PTBS	0.947	2.7

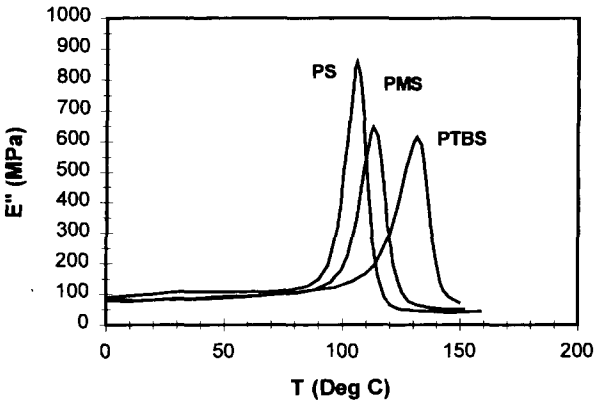

Fig. 6. Flexural loss modulus E'' vs. temperature for PS, PMS and PTBS from dynamic mechanical analysis at 1 Hz with heating rate 2°C min^{-1}.

Table 4
Polydispersity and E'' loss peak half-height width

Polymer	Polydispersity	$\Delta T_{1/2}$/°C
PS	2.09	10
PMS	2.13	12
PTBS	2.31	14

β-and γ-Transitions are very weak and are in the long tails of the glass transitions. An example of PMS data is shown in Fig. 7. The computer program, Peakfit (Jandel Scientific), was used to extract the exact location of these weak transitions. Up to three Lorentzian curves were used to simulate the dispersion of the three observed loss peaks, i.e., glass transition, and β- and γ-transitions. The corresponding Arrhenius plots are represented in Fig. 8. The frequency of T_g was used for the Arrhenius plot

$$\ln f_{max} = \ln f_0 - \Delta H/RT \tag{6}$$

$$\Delta H = -R \times \text{slope} \tag{7}$$

where f_{max} is the frequency at which maximum loss is observed [40,41]. The activation energies thus calculated are listed in Table 5. For β-transitions, the activation energies are all about 17 kcal mol^{-1}. This value matches well the activation energy of β-transition determined by deuterium NMR for polystyrene at 69 kJ mol^{-1} (17 kcal mol^{-1}) [59], although it is different from the values obtained in earlier studies at about 35–40 kcal mol^{-1} [33] and 30 kcal mol^{-1} [40]. The authors believe that the β-transitions observed are due to the local motion of a small section of main chain and thus are similar for all the polymers [40,60]. The γ-transition has an activation energy of 8–10 kcal mol^{-1} (Table 5 and Fig. 8) which is quite close to the literature value 8 kcal

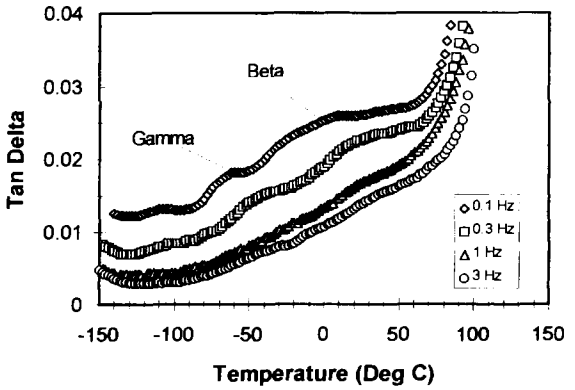

Fig. 7. Expanded view of the β- and γ-transition regions of PMS and their dependence on dynamic mechanical frequency.

mol^{-1} [40]. The small variations among the three polymers can be due to the presence of the methyl group (PMS and PTBS) and the quaternary carbon (PTBS) as shown in Fig. 9. Their rotational activation energies are about 4.2 kcal mol^{-1} [61] and the overall averaged activation energies are lower for PMS at 7 kcal mol^{-1} and PTBS at 8 kcal mol^{-1} compared to that for PS at 10 kcal mol^{-1}.

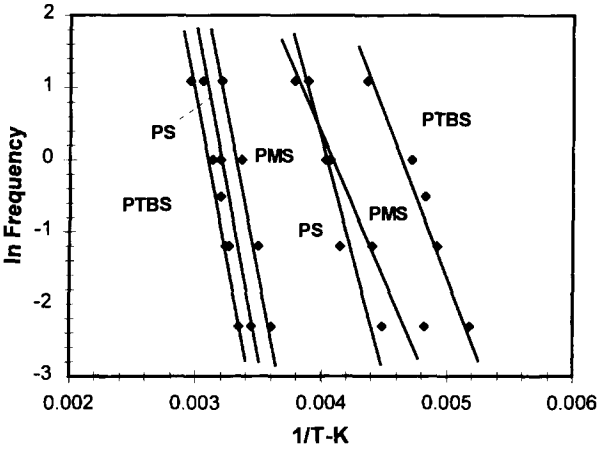

Fig. 8. Arrhenius plots of maximum frequency, ln (frequency) vs. $1/T$, for the β- and γ-transitions of PS, PMS and PTBS.

Table 5
Activation energies for β- and γ-relaxations

Polymer	ΔH_β/ kcal mol^{-1}	ΔH_γ/ kcal mol^{-1}
PS	17	10
PMS	17	7
PTBS	17	8

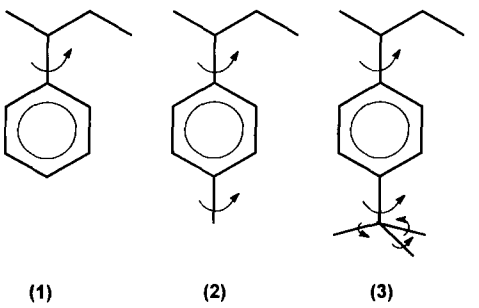

Fig. 9. Rotation modes of side groups of PS (1), PMS (2) and PTBS (3) that give rise to γ-relaxation.

3.3. Glass transition and activation energies by dielectric analysis

Dielectric analysis reveals yet another aspect of the structure-property relations of the polystyrene system. Dielectric analysis is a technique that detects the electrical conductive and capacitive responses of materials. The conductive response is represented by dielectric loss, ε'', which generally is the result of the viscous movement of charge carriers in the polymers, i.e. polar side groups, polar segments of polymer chains, polar guest molecules, and ionic species in the viscous polymeric medium [40–42]. The capacitive response, ε', also known as the dielectric constant, is mainly due to the elastic reorientation of dipoles in the applied electrical field [40,41]. Plots of ε'' are shown in Fig. 10. Furthermore, the frequency dependence of dielectric data can be used to calculate the activation energy of structural transitions and molecular motion by the Arrhenius plot, Fig. 11, based on Eqs. (6) and (7). The glass transition temperatures and their activation energies of the polystyrene system are listed in Tables 6 and 7. The general trend is that the activation energy increases with the glass transition temperature. PTBS is an exception, having a significant increase in the glass transition temperature, ~30°C, yet exhibiting moderate activation energy. Stevens [25] mentioned that two opposing effects on glass transition temperatures and activation energies should be considered when there is para-alkylation: (a) bulky substituents due to branching (widening) of the pendant group generally increase T_g and ΔH; and (b)

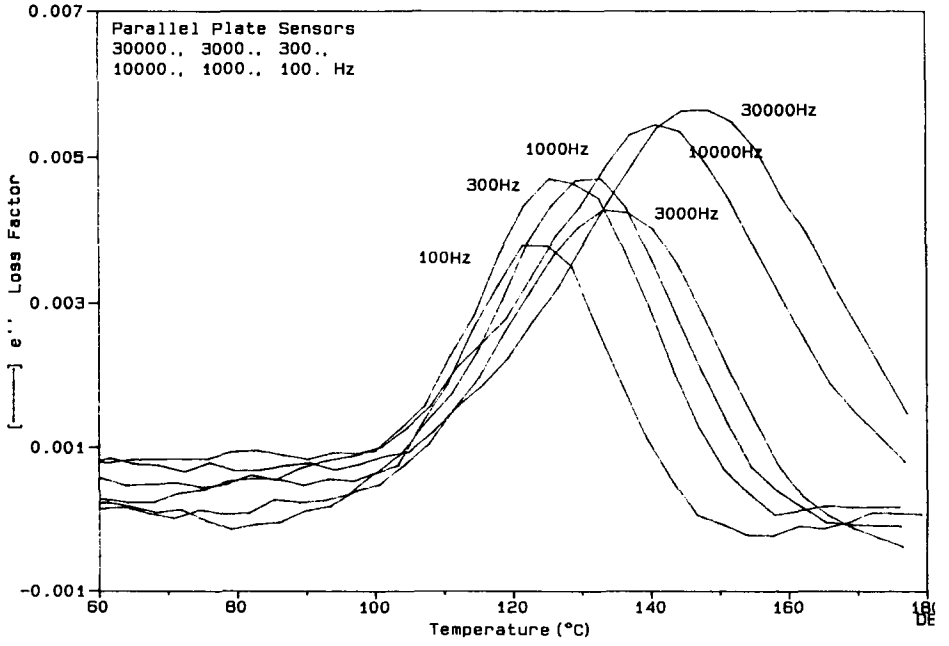

Fig. 10. Dielectric loss ε'' vs. temperature of polystyrene.

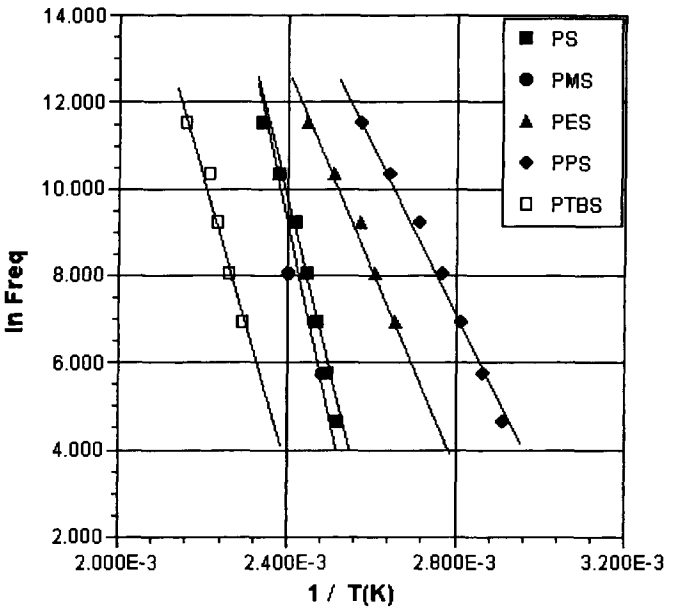

Fig. 11. Arrhenius plots, ln (freq) vs. $1/T$, for the glass transitions of PS, PMS, PES, PPS and PTBS.

Table 6
Glass transition temperatures determined by different methods

Polymers	Creep 5°C step	Stress 5°C step	DSC 5°C min^{-1}	DMA 1 Hz, 2°C min^{-1}	DEA 1 Hz, 3°C min^{-1}
PS	82	87	96.7	106	112
PMS	88	93	101.3	112	118
PES	–	–	64.8	–	79
PPS	–	–	38.5	–	55
PTBS	108	115	125.6	141	148

lengthening of linear pendant groups to a certain point decrease T_g and ΔH. Among the polystyrenes, methyl and *t*-butyl groups have more pronounced branching than lengthening effects, giving higher glass transition temperatures. Ku and Liepins [62] pointed out an additional effect. They believe that higher glass transition temperatures are associated with increased kinetic energy, which is also supported by Matsuoka's conformational relaxation theory [23,24]. This in effect reduces the size of the cooperative segmental movement region and thus the activation energy required for glass transition process is reduced. PTBS with a significantly high T_g exhibits a relative low activation energy.

Table 7
Glass transition activation energies (kcal mol^{-1}) determined by different methods

Polymers	Creep		Stress		DMA		DEA
	ΔH_{C-}	ΔH_{C+}	ΔH_{S-}	ΔH_{S+}	ΔH_{β}	ΔH_{γ}	ΔH_{α}
PS	37	101	44	129	17	10	77
PMS	34	111	36	135	17	7	82
PES	–	–	–	–	–	–	44
PPS	–	–	–	–	–	–	40
PTBS	34	129	34	119	17	8	65

Key: The subscript "C" represents creep and "S" stress relaxation; "+" represents above T_g process and "−" below T_g process.

3.4. *Comparison of transition temperatures and activation energies from different methods*

Tables 6 and 7 list all the transition temperatures and activation energies of the polymers studied in this report, respectively. The transition temperatures observed for all three polymers exhibit the lowest values from creep experiments, followed in increasing order by those from stress relaxations, differential scanning calorimetry, dynamic mechanical analysis and dielectric analysis in our studies. This clearly shows that a kinetic process like the glass transition can have a relative low value when observed from static experiments such as creep and stress relaxation. These low values of T_g are due to the lack of over heating or cooling that is unavoidable in other dynamic processes such as differential scanning calorimetry, dynamic mechanical analysis, dielectric analysis, and even dilatometry. Different processes and different modes of polymeric molecular motion can be detected by different experimental methods as has been demonstrated in our experiments. Low-temperature transitions typically require low activation energies and high-temperature ones require high activation energies. When the glass transition region is approached from different sides, different activation energies are observed corresponding to different modes of molecular motion. However, when the temperature is above the glass transition temperature, the activation energy tends to decrease due to the decreased size of the kinetic unit involved in the relaxation process.

4. Conclusions

The glass transition temperature can be readily obtained from creep and stress relaxation without having to obtain a "rate independent" glass transition temperature from a second method. the glass transition temperature thus obtained is correlated well with literature values determined by isochronal dilatometry. This is believed to be due to the fact that creep and stress relaxation experiments have a static and rate-

independent nature. The glass transition temperatures of creep and stress relaxation separate the whole process into two regions of molecular motion patterens. On the low temperature side, the intramolecular cooperation of small ranges dominates the creep and stress relaxation process. The activation energies associated with this process are determined to be 34–44 kcal mol^{-1}. Above the glass transition temperature, the long-range cooperative segmental main-chain movement is the major mode of motion, which is characterized by elevated activation energies as high as above 101–135 kcal mol^{-1}. Rubbery plateaus of stress relaxation moduli at 250 MPa due to chain entanglement are observed for polystyrene, poly(*p*-methyl styrene) and poly(*p*-*t*-butyl styrene). The flexural storage modulus E' was recorded with dynamic mechanical analysis for polystrene, poly(*p*-methyl styrene) and poly(*p*-*t*-butyl styrene), with an observed density dependency. The peak width of loss modulus E'' is noted as being affected by the molecular weight distribution of each polymer. Two sub-glass-transition temperature transitions, β and γ, were recorded from dynamic mechanical analysis. Their activation energies and modes of motion are interpreted with cooperative movement of monomers of small conformers, and localized phenyl ring and pendant group conformation, respectively. The glass transition processes were best studied by dielectric analysis although secondary transitions were unobservable in these apolar polymers by the dielectric method. The variation in the glass transition temperature and activation energies for the glass transition process were analyzed with regard to steric hindrances due to alkylation.

Acknowledgments

The authors thank Optical Polymer Research Inc. for funding the research. We also extend our thanks to Gregory Schuenemann for preparing poly(*p*-ethyl styrene) and poly(*p*-*n*-propyl styrene) and to Patrick Kelly for helping with GPC measurements.

References

[1] C.G. Overberger, C. Franzier, J. Mandelman and H.R. Smith, J. Am. Chem. Soc., 75 (1953) 3326.
[2] A. Brooks, J. Am. Chem. Soc., 66 (1944) 1295.
[3] M. Sulzbacher and E. Bergmann J. Org. Chem., 13 (1948) 303.
[4] L.L. Ferstandg, J.C. Butler and A.E. Straus, J. Am. Chem. Soc., 76 (1954) 5779.
[5] T.E. Davies, British Plastics, June (1959) 283.
[6] W.G. Barb, J. Polym. Sci., 37 (1959) 515.
[7] D.A. Buckley and P.A. Augostini Polym. preprints, 18 (1977) 528.
[8] A.C. Puleo, N. Muruganandam and D.R. Paul, J. Polym. Sci. Part B, 27 (1989) 2385.
[9] G. Schuenemann, Radiation Stability of Polymers for High Energy Radiation Detectors, M.S. Thesis, University of Florida, 1994.
[10] T. Kaino, M. Fujini and S. Nara, J. Appl. Phys. 52 (1981) 7061.
[11] T. Kaino, J. Polym. Sci. Part A, 25 (1987) 37.
[12] Y. Takezawa, S. Tanno, N. Taketani, S. Ohara and H. Asana, J. Appl. Polym. Sci., 42 (1991) 3195.
[13] Y.Takezawa, N. Teketani, S. Tanno, and S. Ohara, J. Polym. Sci. Part B, 30 (1992) 879.

[14] J.D. Ferry, Viscoelastic Properties of Polymers, 3rd edn, Wiley, New York, 1980.
[15] L.E. Nielsen, R.F. Landel, Mechanical Properties of Polymers and Composites, 2nd. edn., Marcel Dekker, Inc., New York, 1994.
[16] E. Catsiff and A.V. Tobolsky, J. Colloid Sci., 10 (1955) 375.
[17] A.V. Tobolsky, Properties and Structures of Polymers, Wiley, New York, 1960.
[18] H. Leaderman Elastic and Creep Properties of Filamentous Materials and Other High Polymers, Textile Foundation, Washington D.C., 1943.
[19] J.D. Ferry, J. Am. Chem. Soc., 72 (1950) 3746.
[20] M.L.Williams, R.F. Landel and J.D. Ferry, J. Am. Chem. Soc., 77 (1955) 3701.
[21] A.K. Doolittle and D.B. Doolittle , J. Appl. Phys., 31 (1959) 1164.
[22] G. Adam and J.H. Gibbs, J. Chem. Phys., 43 (1965) 139.
[23] S. Matsuoka and X. Quan, Macromolecules, 24 (1991) 2770.
[24] S.Matsuoka, Relaxation Phenomena in Polymers, Hanser Publishers, Munich, 1992.
[25] M.P. Stevens Polymer Chemistry, Oxford University Press, New York, 1990.
[26] I.M. Ward and D.W. Hadley, An Introduction to the Mechanical Properties of Solid Polymers, John Wiley & Sons, Chichester, 1993.
[27] H.H.-D. Lee and F.J. McGarry, Polymer, 34 (1993) 4267.
[28] R.A. Weiss, J.J. Fitzgerald and D. Kim, Macromolecules, 24 (1991) 1071.
[29] J.K. Kim and C.D. Han, Macromolecules, 25 (1992) 271.
[30] A.Y. Gol'dman, translated and edited by M. Shelef and R.A. Dickie, Prediction of the Deformation Properties of Polymeric and Composite Materials, ACS, Washington, DC, 1994.
[31] J.A. Sauer and D.E. Kline, J. Polym. Sci., 18 (1955) 491.
[32] R. Buchdahl and L.E. Nielsen, J. Polym. Sci., 15 (1955) 1.
[33] K.H. Illers, E. Jenckel, Rheol. Acta, 1 (1958) 322.
[34] K.M. Sinnot, Soc. Plastics Engrs. Trans., 2 (1962) 65.
[35] M. Baccaredda, E. Butta and V. Frosini, J. Polym. Sci. Part B, 3 (1965) 185.
[36] R.F. Boyle, Polym. Eng. Sci., 8 (1968) 161.
[37] H. Tenhu, E-L. Heino, J. Appl. Polym. Sci., 44 (1992) 55.
[38] M. Rutkowska, M. Jastrzebska, J-S. Kim and A. Eisenberg, J. Appl. Polym. Sci., 48 (1993) 521.
[39] F. de Candia, G. Romano, R. Russo and V. Vittoria, Colloid Polym. Sci. 271 (1993) 454.
[40] P. Hedvig, Dielectric Spectroscopy of Polymers, John Wiley & Sons, New York, 1977.
[41] N.G. McCrum, B.E. Read and G. Williams, Anelastic and Dielectric Effects in Polymeric Solids, Dover Publications, Inc., New York, 1967.
[42] Y. Feldman and K. Nikolay, Trends in Polymers, 3 (1995) 53.
[43] M. Nozaki, K. Shimada and S. Okamoto, Japan. J. Appl. Phys., 9 (1970) 843.
[44] K. Fukao and Y. Miyamoto, Polymer, 34 (1993) 238.
[45] A.A. Mansour, R. Junge, B. Stoll and W. Pechhold, Colloid Polym. Sci., 270 (1992) 325.
[46] A.A. Mansour and B. Stoll, Colloid Polym. Sci., 272 (1994) 25.
[47] A.A. Mansour, E. Happ, T. Wolf and B. Stoll, Colloid Polym. Sci., 272 (1994) 894.
[48] A. Dhinojwala, G.K. Wong and J.M. Torkelson, J. Chem. Phys., 100 (1994) 6046.
[49] G. Katana, E.W. Fischer, Th. Hack, V. Abetz and F. Kremer, Macromolecules, 28 (1995) 2714.
[50] T. Shimo and M. Nagasawa, Macromolecules, 25 (1992) 5026.
[51] K.C. Rusch, J. Macromol. Sci., Phys. B2, 2 (1968) 179.
[52] G. Halsey, H.J. White and H. Eyring, Text Res. J., 15 (1945) 295.
[53] H.W. Starkweather, Macromolecules, 26 (1993) 4805.
[54] E.B. Baker, R.P. Auty and G.J. Ritenour, J. Chem. Phys., 21 (1953) 159.
[55] J.J. Aklonis, W.J. McKnight and M. Shen, Introduction to Polymer Viscoelasticity, Wiley-Interscience, New York, 1972.
[56] J. Brandrup, in E.H. Immergut (Ed.) Polymer Handboon, John Wiley and Sons, New York, 1989.
[57] R. Rao. J. Chem. Phys., 9 (1941) 682.
[58] D.W. Van Krevelen and P.J. Hoftyzer., Properties of Polymers, Elsevier, Amsterdam, 1970.
[59] J. Zhao, Y.H. Chin, Y. Liu, A.A. Jones, D.T.Inglefield, R.P. Kambour and D.White., Macromolecules, 28 (1995) 3881.

[60] V.A. Bershtein., Differential Scanning Calorimetry of Polymers; Physics, Chemistry, Analysis, Technology, Ellis Horwood, New York, 1994.
[61] M. Gordon, High Polymers, Iliffe Books, London, 1963.
[62] C.C. Ku and R. Liepins, Electrical Properties of Polymers, Chemical Principles, Hanser Publishing, 1987.